Journal of Polymers and the Environment (2022) 30:3209–3217
https://doi.org/10.1007/s10924-022-02427-z

ORIGINAL PAPER

Highly toughening modification of Hyperbranched polyester with environment-friendly caprolactone as end group on poly(3-hydroxybutyrate-co-3-hydroxyvalerate)

Xiaolong Han[1,2] · Yujuan Jin[1,2] · Jian Huang[1,2] · Huafeng Tian[1,2] · Maolin Guo[1,2]

Accepted: 7 March 2022 / Published online: 22 March 2022
© The Author(s), under exclusive licence to Springer Science+Business Media, LLC, part of Springer Nature 2022

Abstract

Hyperbranched polymer with flexible long chains (Ɛ-CL) were synthesized based on hydroxyl terminated hyperbranched polyesters (HBPEs). The prepared HBP-CLs were used to toughen poly(3-hydroxybutyrate-co-3-hydroxyvalerate) (PHBV) by melt-blending. Comparing with pure PHBV, the crystallinity (X_c) of the PHBV/3.0phr HBP-CLs blends decreased by 10.2% (from 67.8 to 60.9%), the impact strength increased by 533.3% (from 5.1 kJ·m^{-2} to 32.3 kJ·m^{-2}), and the elongation at break increased by 160.5% (from 1.62 to 4.22%). With the increase of HBP-CLs, the fracture surface of the PHBV/HBP-CLs blends became rough and a significant decrease in crystallization area can be seen from POM images. Even filamentous structures and tiny holes was formed, which further demonstrated that HBP-CLs acted as an excellent toughening effect on PHBV.

Keywords Poly(3-hydroxybutyrate-co-3-hydroxyvalerate) (PHBV) · Biodegradable · Hyperbranched polymer · Toughening

Introduction

In recent years, a lot of research groups have focused on bio-sourced and biodegradable materials for the purpose of reducing environmental pollution of non-degradable polymer wastes such as plastic materials 1, 2. Biodegradable polymer materials have been proposed as potential and suitable replacements for traditional plastics as they present good processing properties and a much lower environmental impact 3, 4. Therefore, the applications of biodegradable polymers have increased in the last decade. For example, poly(lactic acid) (PLA) can be used for food packaging 5, 6, while poly(glycolic acid) (PGA), poly(e-caprolactone) (PCL) 7, poly(hydroxybutyrate) (PHB) can be used to fabricate scaffolds in tissue engineering. Among all the biodegradable polymers produced from renewable resources, poly(hydroxyalkanoates) (PHAs) have a very wide range of properties and applications 8, 9. They are synthesized intracellularly by bacteria from agricultural raw materials as a source of carbon and energy 10.

Poly(3-hydroxybutyrate) (PHB) and its copolymer with valerate poly(3-hydroxybutyrate-co-3-hydroxyvalerate) (PHBV) have received considerable scientific attention as green materials among available biodegradable materials 11, 12. PHBV is a natural thermoplastic polyester that is produced by a species of bacteria 13. PHBVs are one of the most commonly used high performance biopolymers. Moreover, PHBV is a suitable candidate for biomedical uses due to its natural origin, biocompatibility, biodegradability, as well as tunable mechanical properties. However, large-scale use of PHBV is restricted by its brittleness 14, thermal instability, and narrow processing window 15. There are several reports on blending PHBV with flexible polymers, such as poly (butylene succinate) (PBS), poly (butylene

✉ Yujuan Jin
jinyujuan@th.btbu.edu.cn

✉ Huafeng Tian
tianhuafeng@th.btbu.edu.cn

[1] School of Chemistry and Materials Engineering, Beijing Technology and Business University, 100048 Beijing, P. R. China

[2] Beijing Key Laboratory of Quality Evaluation Technology for Hygiene and Safety of Plastics, Beijing Technology and Business University, 100048 Beijing, P. R. China

adipate-co-terephthalate) (PBAT), natural rubber (NR) 16. Therefore, blending is an industrially viable and cost effective way to improve its toughness 17, 18.

Poly(e-caprolactone) (PCL) is a semi-crystalline linear aliphatic polyester derived from the ring opening polymerization of e-caprolactone. It is a biodegradable, biocompatible, and nontoxic polyester with excellent mechanical strength 19. PCL is often used to construct the soft segment structure of copolymers 20, 21, whose unstable aliphatic ester bonds can be hydrolyzed, and the degradation product 6-glycolic acid is a non-toxic metabolite 22.

Hyperbranched polymers (HBPs), which are polymerized with polyfunctional monomers, represent a new polymer form developed in the past 30 years 23. Compared with linear polymers, HBPs have many unique advantages such as the three-dimensional (3-D) globoid-like structure, a high density of active terminal functional groups at the periphery, abundant internal cavities inside, many branch points, and a low probability of molecular chain entanglement 24, 25. Therefore, HBPs are applied in multiple fields such as medicine, biology, engineering and materials 26, 27. Compared with a conventional small molecular modifier, macromolecular HBPs cannot easily be separated out and migrate. In recent years, more and more attention has been paid to improve the properties of polymers by using HBPs as a modifier. The reported 28 literatures have indicated that if the terminal functional groups of a HBP were used as a proton donor or receptor to act on the resin, hydrogen bonding would be generated among the molecules of the blended polymers. Hydrogen bonding influences several properties of polymeric blends, such as the blending efficiency, glass transition temperature (T_g), melting point, crystallization, and surface energy, etc.

In this work, HBPs with highly branched three-dimensional structure and Ɛ-CL (ring-opening) with good flexibility were combined to synthesize the end-flexible long-chain hyperbranched polymer (HBP-CLs) through structural design. Then it was used to blend with PHBV and the results indicated that HBP-CLs was a good toughening modifier of PHBV.

Experimental

Materials

Trimethylolpropane (TMP) and p-toluenesulfonic acid (p-TSA) were purchased from Shanghai Macklin Biochemical Co., Ltd. (Shanghai, China). Dimethylolpropionic acid (DMPA) and Stannous octoate (Sn $(Oct)_2$) were purchased from Shanghai Aladdin Biochemical Technology Co., Ltd. (Shanghai, China). Ɛ-Caprolactone (Ɛ-CL) was purchased from Aladdin Industrial Corporation (Shanghai, China). Methyl alcohol (MeOH) was purchased from Beijing Chemical Works (Beijing, China). Tetrahydrofuran (THF) was purchased from Beijing Chemical Works (Beijing, China). PHBV (Y1000P) was supplied by Ningbo Tian'an Biological Materials Co., Ltd. (Ningbo, Zhejiang Province, China).

Synthesis of HBPEs and HBP-CLs

HBPEs with generation 3 (G3 HBPEs) were prepared by "one step" method according to an established synthetic scheme 29 using Trimethylolpropane (TMP) and Dimethylolpropionic acid (DMPA) as basic raw materials. The 2.58 g prepared HBPEs was accurately weighed and placed in three flasks, heated and melted in a water bath at 100℃, and the mechanical stirring speed was set to 60 rpm. After being completely melted, it was connected to the vacuum tube for vacuum drying for 6 h, and the water was fully dried. After removing the vacuum, 3–4 drops of $Sn(Oct)_2$ were added into the flask, then the temperature was raised to 110 ℃ and the rotational speed was set to 120 rpm, and then 54.21 g Ɛ-CL was added for continuous reaction for 24 h to obtain a viscous liquid. After that, it was dissolved into THF, cold MeOH precipitated polymer was added and filtered while it was cold, and the white powder was obtained by vacuum drying, which was the target product, HBP-CLs,

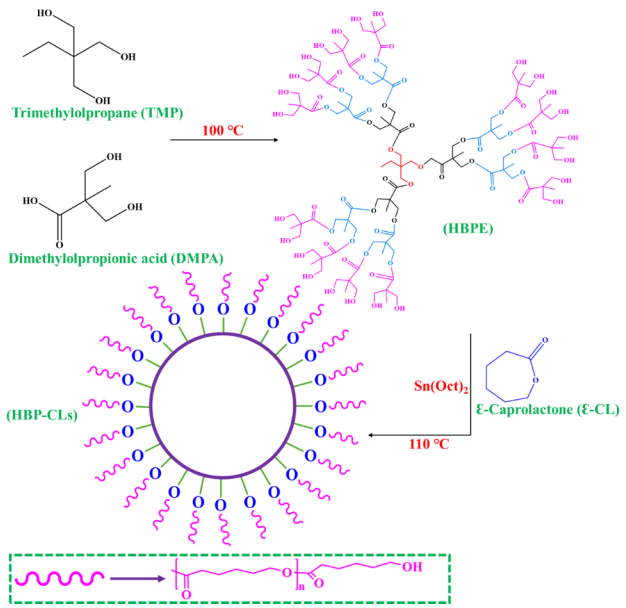

Fig. 1 Synthesis and structure characterization of HBPEs and HBP-CLs

and the yield was 95.72%30. Figure 1 shows the process and detailed chemical structure of the prepared HBP-CLs.

Preparation of the blends

PHBV/HBP-CLs blends were prepared by mixing PHBV and HBP-CLs (0, 1, 2, 3, 4, 5, 6 phr) in internal mixer (XSS-300, MARS Rheomix, China) at 180 °C. The pellets were first poured into the heating chamber. The initial blending speed was set at 20 rpm. After the polymer pellets fully melted (usually takes 1 min), the speed was increased to 60 rpm and lasted for 8 min. For the purposes of comparison, pure PHBV resins were also melt-blended under the same processing conditions. The blends were then cooled down to room temperature before crushing and granulating through a Crushing Machine (HP-150, Beijing Huanyatianyuan Mechanical and Technical Co., Ltd.). The blend films were prepared using the thermal molding method with the temperature 180 °C, the number of exhausts 8 times, and the time 30s.

Characterization

Fourier transform infrared spectroscopy (FT-IR)

Samples were mixed with KBr at a weight ratio of 1:100 and processed into pellets for the use in FT-IR measurements and to aid the possible correlation between the intensities of absorption bands and the quantity of corresponding functional groups. FT-IR spectra of HBPEs and HBP-CLs were recorded using a FT-IR spectrometer (Nicolet iZ10, Thermo Scientific, American) and FT-IR spectra were recorded in the range of 4000–500 cm^{-1} with a resolution of 4 cm^{-1} and 50 scans.

Nuclear magnetic resonance (NMR)

^{1} H and ^{13} C high-resolution one-dimensional NMR spectra were recorded at room temperature in Chloroform-d ($CDCl_3$) using an NMR spectrometer (Agilent NMR Magnet).

Differential scanning calorimetry (DSC)

A differential scanning calorimeter (Q100, TA, USA) was used to investigate the melting and non-isothermal crystallization of the blends. Samples of 5–10 mg were encapsulated in aluminum pans and heated from − 50 to 200 °C at a heating rate of 10 °C /min and cooled from 200 °C to -50 °C at a cooling rate of 20 °C /min using nitrogen as purge gas. The thermal history of the samples was erased by a preliminary heating (room temperature to 200 °C range). The measurements were made from the first cooling scan and the second heating scan. The degree of crystallinity (X_c) of PHBV/HBP-Bs blends was calculated according to Eq. (1):

$$X_c = \frac{\Delta H_m}{(1 - \varnothing_{HBP-CLs})\,\Delta H_{100\%PHBV}} \times 100\% \quad (1)$$

where ΔH_m is the melting enthalpy, $\varnothing_{PHBV-CLs}$ is the weight fraction of HBP-CLs,

$\Delta H_{100\%\ PHBV}$ is the melting enthalpy of pure PHBV ($\Delta H_{100\%\ PHBV} = 146.6\ J{\cdot}g^{-1}$)31.

Thermogravimetric analysis (TGA)

Thermal stability of blends was performed using a TGA apparatus (Q-50, TA, USA). The sample weight was approximately 5 mg. Experiments were performed in the temperature range room temperature to 700 °C at a heating rate of 20 °C /min under nitrogen atmosphere.

Polarized Optical Microscopy (POM)

The crystallization behavior of neat PHBV and PHBV/HBP-CLs blends was studied by a POM (CBX51, Olympus, Japan) equipped with a Linkam hot stage (THMS600/HFS91). Samples were heated to 200 °C at a heating rate of 50 °C /min between two glass slides and then equilibrated at this temperature for 5 min to eliminate any residual PHBV crystallization seeds, then cooled to room temperature at a nature cooling rate. During the cooling process, crystallization processes of PHBV and PHBV/HBP-Bs blends were observed respectively.

Mechanical properties

Tensile strength and elongation at break of the blends were tested by a computer-controlled electronic universal testing machine (CMT6104, MTS Industry System Co., Ltd., Shenzhen, Guangdong Province, PR China) according to ISO 527-2:2016 in rate of 5 mm/min. The size of the spline was determined according to the ISO 527-2:2016: dumbbell-type spline, L = 150 mm, d = 4 mm.

Impact strength was tested by an electronic Izod impact testing machine (XJUD-5.5, Chengde Jinjian Testing Instrument Co., Ltd., Chengde, Hebei Province, PR China) according to ISO180:2000 with 1 J of the impact energy. The size of the A-type notched spline was determined according the ISO180:2000: 80 mm×10 mm×4 mm.

Scanning electron microscope (SEM)

The microscopic morphology of the impact section of the specimen was observed by scanning electron microscopy (Quanta FEG, FEI, USA) at environmental mode. All specimens were sputter-coated with a thin layer of gold.

Results and discussion

Structure analysis of HBP-CLs

The FTIR spectra of HBPE and HBP-CLs were shown in Fig. 2 (a). The FTIR spectra of the intermediate product HBPEs and the target product HBP-CLs were compared. It can be seen that there was a characteristic absorption peak connected by multiple (more than four) -CH_2- in the spectrum of HBP-CLs at 731 cm^{-1}, indicating the flexible long chain. The absorption peak around the 3500 cm^{-1} was the hydroxyl absorption peak. The bands near 1730 cm^{-1} corresponded to C = O stretching vibrations. The hydroxyl absorption peak in the HBP-CLs spectrum became narrower and weaker. Thus it could be concluded that the hydroxyl end groups became dispersed and were not easy to form hydrogen bonds with each other, which indicated that the flexible long chain had been grafted to the hydroxyl end of HBPEs. From the analysis of infrared results, the target product HBP-CLs was synthesized successfully.

The further analysis of the molecular structure of HBP-CLs by ^{13} C-NMR and ^{1} H-NMR were shown in Fig. 2 (b) and (c). As shown in Fig. 2(b), the chemical shift at 173.53ppm was the vibrational absorption peak of the C atom on the ester group of HBP-CLs. The chemical shift at 77.24 ppm was the vibrational absorption peak of C atom on solvent $CDCl_3$. The chemical shift at 64.14ppm was the vibrational absorption peak of the C atom on the methylene group connected to the ester group. And the chemical shift at 25.54ppm was the vibrational absorption peak of the C atom on the methylene group on the long chain. The chemical shift at 34.12ppm was the vibrational absorption peak of the C atom on the methylene group connected to the ester group and belongs to the long chain.

The ^{1} H-NMR diagram of HBP-CLs and the detailed structure was shown in Fig. 2 (c) and (d). The chemical shift at 1.40 ppm was the vibrational absorption peak of the H atom on the methylene (-CH_2-CH_2-OH) connected to the hydroxyl terminal, the chemical shift at 1.66ppm was the vibrational absorption peak of the H atom on the methylene (-CH_2-) on the flexible long chain. The chemical shift at 2.32ppm was the vibrational absorption peak of the H atom on the methylene (-CH_2-CH_2-CO-O-) connected to the ester group. The chemical shift at 3.66ppm was the vibrational absorption peak of H atom on the methylene (-CH_2-OH) connected to the terminal hydroxyl. The chemical shift at 4.08ppm was the vibrational absorption peak of H atom on methylene (-CH_2-O-CO-) connected to carbonyl group, and the chemical shift at 7.28ppm is the vibrational absorption peak of H atom on solvent $CDCl_3$. Based on the analysis of the above NMR results, the target product HBP-CLs was synthesized successfully.

Thermal properties

The DSC curves of PHBV, PHBV/HBP-CLs blends and HBP-CLs were shown in Fig. 3 (a) and (b), while the relevant data was shown in Table 1. Fig. 3 (a) and (b) showed the first cooling and second heating processes of PHBV, PHBV/HBP-CLs blends and HBP-CLs.

The crystallization temperature (T_c) of the blends decreased at first and then increased with the addition of HBP-CLs, from 121.15 ℃ of pure PHBV to 116.06 ℃ of PHBV/HBP-CLs blends with the HBP-CLs content of 3.0 phr. The melting temperature (T_m) decreased slightly, but they were generally around 170 ℃. The crystallinities (X_c) decreased from 67.87% of pure PHBV to 60.94% of 3.0phr. The T_c and T_m of pure HBP-CLs was 20.73 ℃ and 50.08 ℃. The decrease of T_c indicated that crystallization became more difficult.

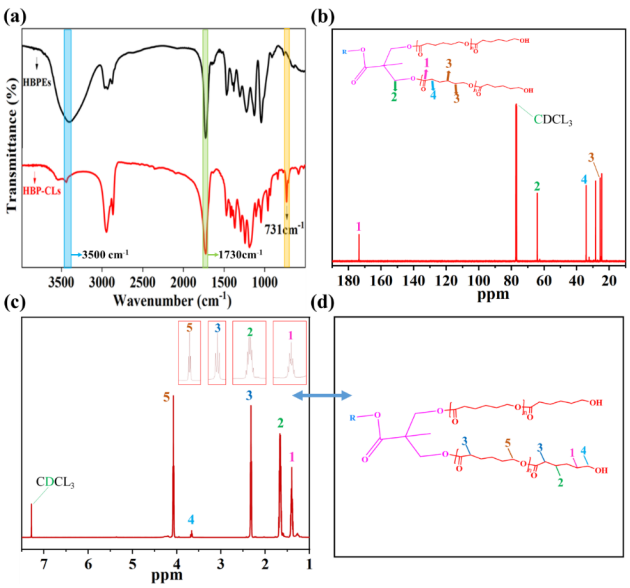

Fig. 2 FTIR spectra of the intermediate HBPEs and target HBP-CLs **(a)**. The ^{13} C-NMR **(b)** and ^{1} H-NMR **(c)** spectrogram of HBP-CLs. **(d)** is the detailed structure

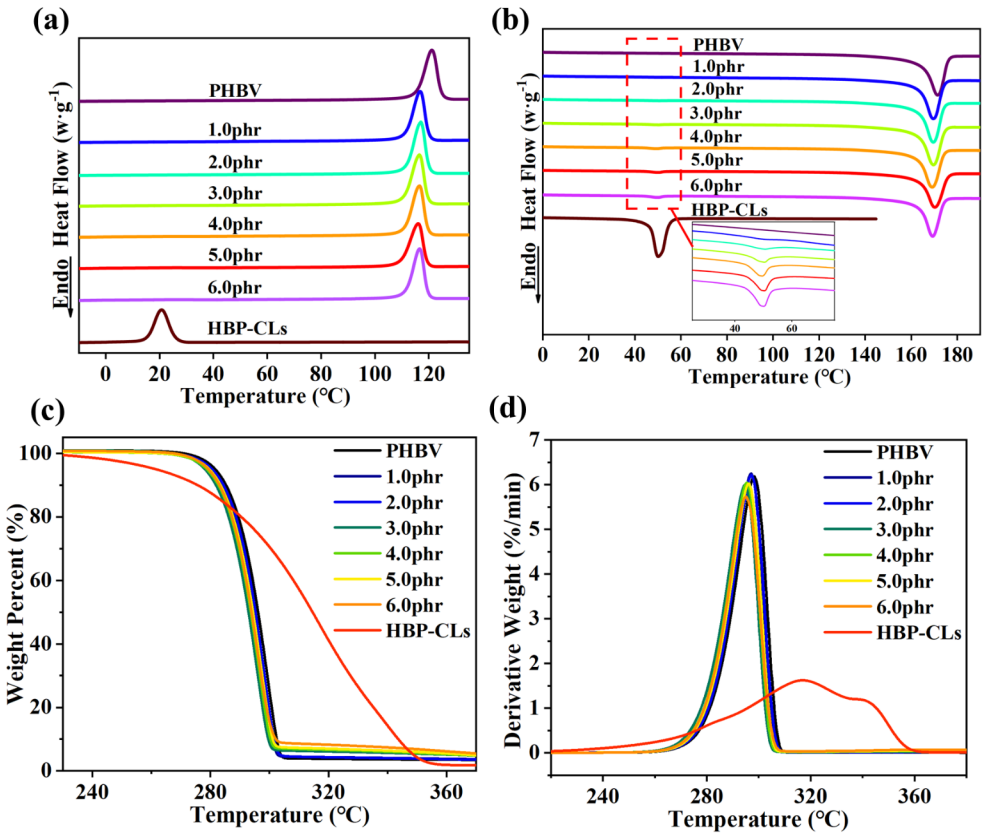

Fig. 3 Thermal properties of neat PHBV and the PHBV/HBP-CLs blends

The decrease of X_c may be due to the entanglement between the long flexible chain at the end of HBP-CLs and the molecular chain of PHBV. The micro-crosslinking structure limited the movement of PHBV molecular chain. At the same time, there were hydroxyl groups at the end of the flexible long chain of HBP-CLs, and the hydrogen bonding interaction between that hydroxyl groups and the ester groups on the PHBV molecular chain limited the movement of the molecular chain. Therefore, the synergistic effect of flexible long chain entanglement and hydrogen bond reduced the crystallinity. However, when the content of HBP-CLs exceeded that of 3.0phr, the crystallinity of PHBV/HBP-CLs blends began to increase.

The reason was that with the addition of excessive HBP-CLs, the flexible long chains of HBP-CLs molecules were entangled with each other, which led to their agglomeration. Therefore, this phenomenon affected the dispersion effect of HBP-CLs in PHBV.

(a)DSC curves by cooling scan **(b)** DSC curves by second heating scan.

(c) TGA curves **(d)** DTG curves.

POM

The POM images of neat PHBV and the PHBV/HBP-CLs blends with different contents of HBP-CLs were shown

Table 1 DSC and TG data sheet of PHBV and PHBV/HBP-CLs blends

Samples	T_c (°C)	T_m (°C)	X_c (%)	$T_{5\%}$ (°C)	$T_{50\%}$(°C)
PHBV	121.1	171.4	67.8(±0.4)	281.6	296.1
1.0phr	117.0	169.6	64.3(±0.3)	280.3	295.0
2.0phr	116.5	169.5	64.1(±0.2)	280.5	295.2
3.0phr	116.0	169.0	60.9(±0.1)	278.1	292.9
4.0phr	116.0	169.2	61.2(±0.2)	278.7	293.6
5.0phr	116.5	169.5	62.3(±0.4)	279.5	294.4
6.0phr	116.0	170.2	62.8(±0.3)	279.3	293.9
HBP-CLs	20.7	50.0	-	261.4	314.6

The thermogravimetric analysis (TGA) and derivative thermogravimetry (DTG) curves of PHBV/HBP-CLs blends with different HBP-CLs contents and HBP-CLs were shown in Fig. 3 (c) and (d). The temperatures with weight loss of 5% ($T_{5\%}$) and 50% ($T_{50\%}$) were listed in Table 1. It can be found from Fig. 3 (c) and (d) that the thermal degradation of blends had only one thermal decomposition stage, showing a typical "Z" shape. The initial decomposition temperature of the blends did not change obviously and the difference was about 1–2 °C. The second pyrolysis peak moved towards to low temperatures with the increase of HBP-CLs content, which indicated that the thermal stability of blends decreased with the increase of HBP-CLs content. With the increase of the PHB-CLs contents, temperature at 50% weight loss ($T_{50\%}$) gradually decreased from 296.1 °C for neat PHBV to the maximum of 292.9 °C for the blends with 3.0phr HBP-CLs and then increased slightly to 294.4 °C for the blends with 5.0phr HBP-CLs. The similar trend was also observed for temperature at 5% weight loss ($T_{5\%}$), which was ascribed to poor crystallization ability and the formation of imperfect crystals. But on the whole, the addition of HBP-CLs did not affect the thermal workability of the blends

in Fig. 4 (a-h). With the increase of HBP-CLs (less than 3.0phr), the number of crystals in PHBV/HBP-CLs blends decreased gradually and the crystallization area decreased. When the content of HBP-CLs was 3.0phr, the crystal number and crystallization region of PHBV/HBP-CLs blends were the least, indicating that the addition of HBP-CLs inhibited the formation of PHBV crystal nucleus and reduced its crystallinity.

With the increase of HBP-CLs content, the spherulite structure of the blends slowly changed from annular spherulite to radial spherulite. One of the changes in spherulite structure was due to the good compatibility of PHBV and HBP-CLs as well as the result of intermolecular interaction. This phenomenon was more obvious when the content of HBP-CLs continued to increase. When the content of HBP-CLs continued to increase, the crystallinity of the blends tended to increase. The reason for the decrease of crystallinity has been mentioned earlier in Thermal properties.

HBP-CLs content: **(a)** 0phr; **(b)** 1phr; **(c)** 2phr; **(d)** 3phr; **(e)** 4phr; **(f)** 5phr;

(g) 6phr; **(h)** pure HBP-CLs.

Mechanical properties

Figure 5 showed the mechanical properties of the PHBV and PHBV/HBP-CLs blends with different content of HBP-CLs. The tensile strength (Fig. 5a) decreased slightly with the addition of HBP-CLs. It can be seen that the addition of HBP-CLs had a good toughening effect on PHBV without affecting the tensile strength significantly. Meanwhile, the elongation at break (Fig. 5a) of the PHBV-CLs blends were increased by 160.5%, from 1.62 to 4.22%, when the content of HBP-CLs was 3.0 phr. As shown in Fig. 5(b), the impact strength of the PHBV/HBP-CLs blends increased firstly and then decreased upon addition of HBP-CLs. The impact strength of the PHBV/HBP-CLs blends with 3.0phr content of HBP-CLs was increased by 533.3%, from 5.1 kJ/m^{-2} of the pure PHBV to 32.3 kJ/m^{-2}. This suggests that a strong adhesion between the toughening phase (HBP-CLs) and the matrix (PHBV) existed in the blends, resulting in an efficient dispersion of the HBP-CLs and efficient stress transfer at the interface. These improvements could be attributed to the restrained chain movement and refined crystalline structure during the deformation due to chain entanglements (entanglement occurs between the flexible long chains of HBP-CLs and the molecular chains of PHBV) and hydrogen bonding interactions (hydrogen bonding occurs between the spherical outer hydroxyl group of HBP-CLs and the carbonyl group in the PHBV molecular chain). However, once the HBP-CLs contents exceeded 3phr, slight decreases in the elongation to break and impact strength occurred because of

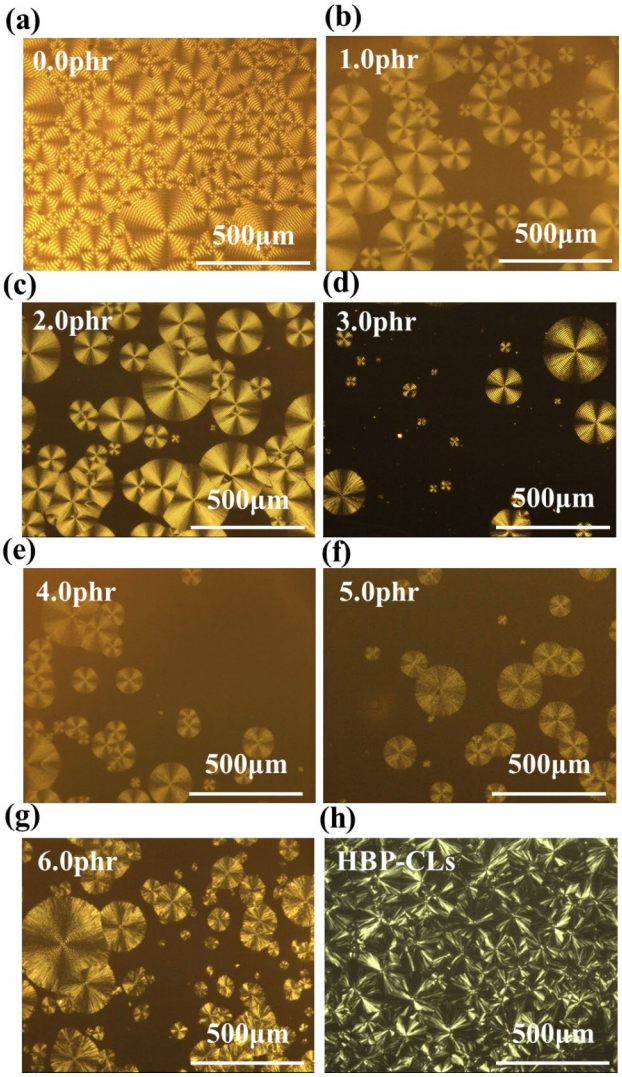

Fig. 4 POM of neat PHBV and the PHBV/HBP-CLs blends

slight HBP-CLs agglomeration, which could be supported by the SEM observations.

Figure 5 (c) was the stress-strain curves of blends. The toughness of PHBV had been significantly improved after adding HBP-CLs. With the increase of HBP-CLs content, the toughness first increased and then decreased, and reaching the maximum when HBP-CLs content was 3.0phr. Figure 5 (d) was the integral area under the stress-strain curve of blends, which was the tensile toughness (τ) and it was calculated by Eq. (2):

$$\tau = \sum_{\epsilon_x=0}^{\epsilon_x=\epsilon_b} \sigma \epsilon_x \tag{2}$$

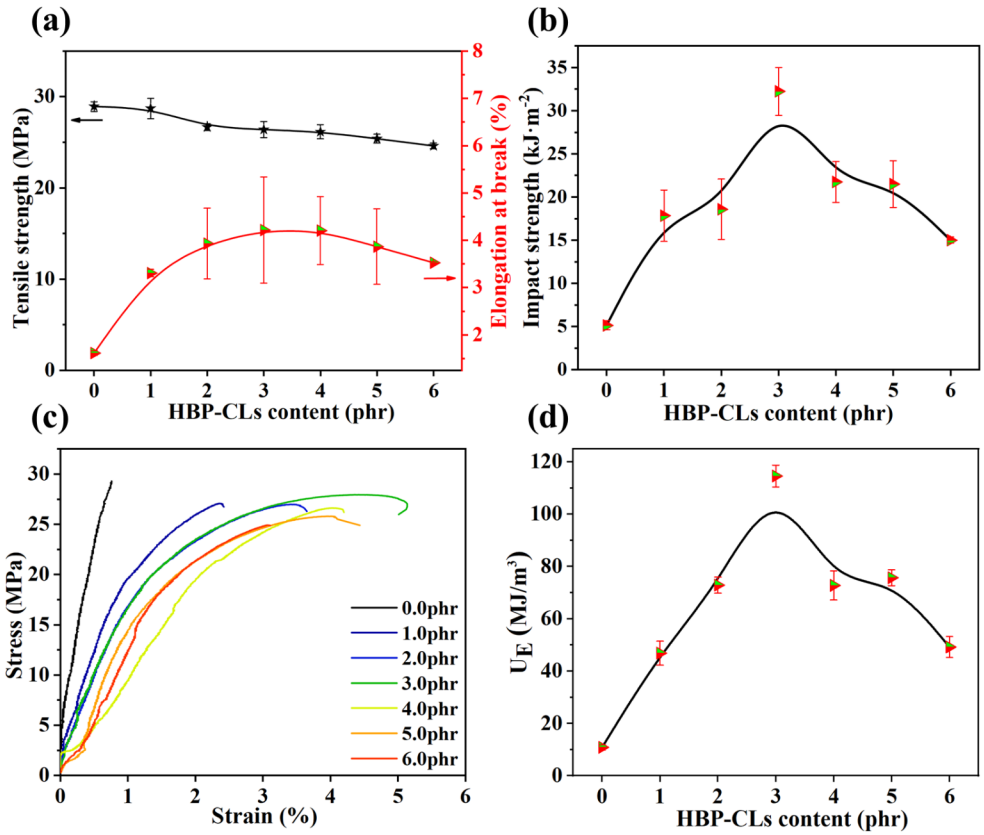

Fig. 5 Mechanical properties of PHBV and PHBV/HBP-CLs blends

As can be seen in the figures, the tensile toughness (τ) was improved after adding HBP-CLs, and reaching the maximum when HBP-CLs content was 3.0phr.

a. **(a)** Elongation at break and Tensile strength. **(b)** Impact strength.
b. **(c)** Stress-strain curves. **(d)** Tensile toughness..

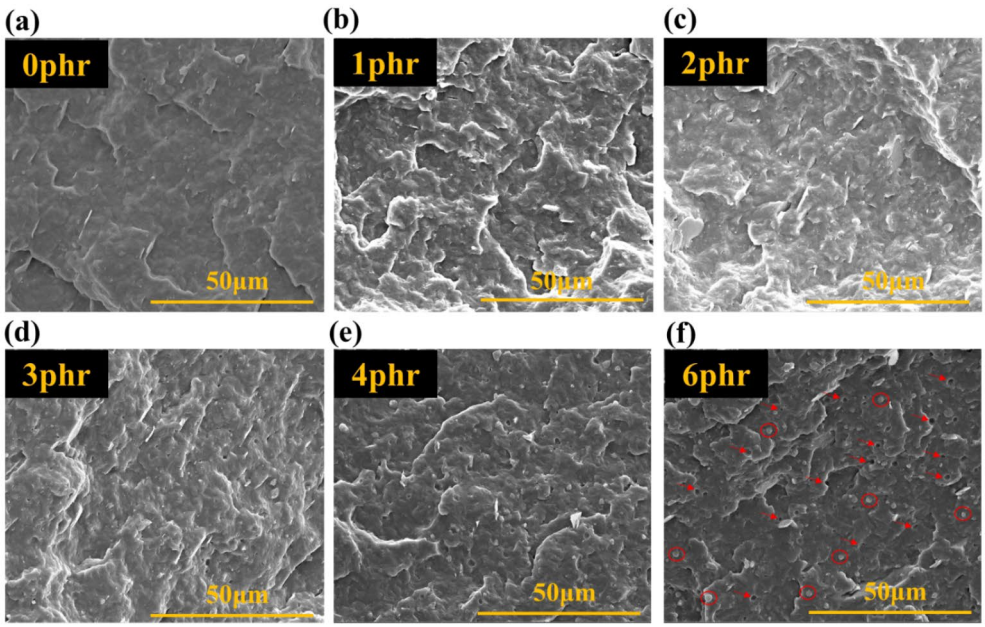

Fig. 6 SEM of impact section of PHBV and PHBV/HBP-CLs blends

SEM

Figure 6 showed the SEM images of the impact fracture morphology of the pure PHBV and PHBV/HBP-CLs blends. Figure 6 (a) was a micrograph of the impact section of pure PHBV, from which it can be seen that the cross section was relatively smooth and showed brittle fracture. The impact section began to become rough with the addition of HBP-CLs, indicating that the toughness was improved as shown in Fig. 6(b)-(f). In addition, there were some tiny holes in the cross section, which was formed by the debonding between PHBV matrix and HBP-CLs particles. And there was a certain plastic deformation, which was also a manifestation of toughness. However, the surface of the blend presented a fuzzy and mushy appearance with further increase of HBP-CLs (higher than 3.0phr). It's obvious that the small hole was getting bigger (the red arrows). This phenomenon indicated that excessive HBP-CLs was wrapped on the surface of the blends and certain agglomeration appeared (the red circles), which would damage the mechanical performances.

The modification mechanism

The sketch for the formation of hydrogen bonding interaction and evolution of polymer aggregation structure and crystal structure in the PHBV/HBP-CLs blends was shown in Fig . 7 (a). The toughening effect of HBP-CLs on PHBV can be summarized into follow aspects: (1) HBP-CLs and PHBV are uniformly mixed, and a large number of flexible long chains at the end of HBP-CLs were entangled with PHBV molecular chains to form a certain microcrosslinking structure with the HBP-CLs molecular core as the center. The joint action of chain entanglement and cocrystallization affects the directional arrangement of PHBV molecular chains.

(2) The hydroxyl group at the end of the flexible long chain interacted with the ester group on the PHBV molecular chain because of the hydrogen bonding, which restricted the movement of the PHBV molecular chains. In order to show more clearly, the infrared spectra of pure PHBV and PHBV/3.0phrHBP-CLs blends are selected as a comparison, as shown in Fig. 7 (b). The terminal hydroxyl group in HBP-CLs interacted with the ester group on the PHBV molecular chain. The formation of hydrogen bond reduced the electron cloud density and chemical bond force constant, thus reducing the stretching vibration frequency. That is, it can be seen that the ester group peak of PHBV/3.0phrHBP-CLs blends moved to low wavenumber (from 1730.32 cm^{-1} to 1725.28 cm^{-1}).

(3) In addition, the three-dimensional network structure of HBP-CLs uniformly dispersed in the blend absorbed the impact energy of external force and achieved the effect of toughening.

Conclusions

In this work, HBP-CLs that had flexible long chains was successfully synthesized and used as a modifier for the toughening of PHBV. The studies of thermal performance showed the addition of HBP-CLs had a greater impact on the T_c and did not affect the T_m. The T_c tended to decrease at first and then increase. The initial decomposition temperature of the blends did not change obviously and there was only one thermal decomposition stage. The impact fracture surface of the PHBV became rough with the addition of HBP-CLs according to the SEM images, and even obvious filamentous structure and tiny holes could be seen. The addition of HBP-CLs did decrease the crystallinity of PHBV according to the POM images, which made it possible to toughen PHBV. The elongation at break and impact strength of PHBV were greatly improved without the sacrifice of tensile strength. The results indicate that the formation of micro-crosslinking structure and hydrogen-bond interaction played a critical role in toughening process of PHBV. In summary, HBP-CLs was an effective additive to toughen PHBV.

Acknowledgements The authors are grateful to the financial support of Beijing Young Top-notch Personnel Foundation (CIT&TCD201804030), Beijing Key Project of Natural Science (KZ201810011017), School Level Cultivation Fund of Beijing Technology and Business University for Distinguished and Excellent Young Scholars (BTBUYP2021), and Open Fund of Beijing Key Laboratory of Quality Evaluation Technology for Hygiene and Safety of Plastics (Beijing Technology and Business University).

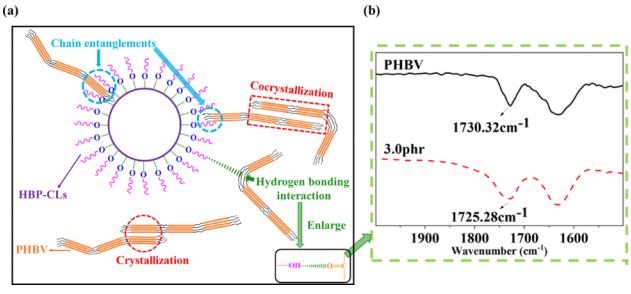

Fig. 7 (a) Sketch for the formation of hydrogen bonding interaction and evolution of polymer aggregation structure and crystal structure in the PHBV/HBP-CLs blends. (b) FT-IR curves of PHBV and 3phr blends

References

1. Ashori A, Jonoobi M, Ayrilmis N et al (2019) Preparation and characterization of polyhydroxybutyrate-co-valerate (PHBV) as green composites using nano reinforcements. Int J Biol Macromol 136:1119–1124
2. Deeksha B, Sadanand V, Hariram N et al (2021) Preparation and properties of cellulose nanocomposite fabrics with in situ generated silver nanoparticles by bioreduction method. J Bioresour Bioprod 6(1):75–81
3. Alaerts L, Augustinus M, Van Acker K (2018) Impact of Bio-Based Plastics on Current Recycling of Plastics. Sustainability 10(5):1487. DOI: https://doi.org/10.3390/su10051487
4. Ashok B, Hariram N, Siengchin S et al (2020) Modification of tamarind fruit shell powder with in situ generated copper nanoparticles by single step hydrothermal method. J Bioresour Bioprod 5(3):180–185
5. Siracusa V, Rocculi P, Romani S et al (2008) Biodegradable polymers for food packaging: a review. Trends Food Sci Tech 19(12):634–643
6. Braga NF, da Silva AP, Arantes TM et al (2018) Physical–chemical properties of nanocomposites based on poly(3-hydroxybutyrate-co-3-hydroxyvalerate) and titanium dioxide nanoparticles. Mater Res Express 5(1):015303. DOI: https://doi.org/10.1088/2053-1591/aa9f7a
7. Liu H, Gao Z, Hu X et al (2016) Blending Modification of PHBV/PCL and its Biodegradation by Pseudomonas mendocina. J Polyme Environ 25(2):156–164
8. Pillin I, Montrelay N, Bourmaud A et al (2008) Effect of thermo-mechanical cycles on the physico-chemical properties of poly(lactic acid). Polym Degrad Stabli 93(2):321–328
9. Ibrahim MI, Alsafadi D, Alamry KA et al (2020) Properties and Applications of Poly(3-hydroxybutyrate-co-3-hydroxyvalerate) Biocomposites. J Polyme Environ 29(4):1010–1030
10. Rivera-Briso AL, Serrano-Aroca A (2018) Poly(3-Hydroxybutyrate-co-3-Hydroxyvalerate): Enhancement Strategies for Advanced Applications. Polymers 10(7):732. DOI: https://doi.org/10.3390/polym10070732
11. Zhang X, Zhang J, Xu J et al (2018) Engineering Escherichia coli for efficient coproduction of polyhydroxyalkanoates and 5-aminolevulinic acid. J Ind Microbiol Biotechnol 45(1):43–51
12. Wagner A, Poursorkhabi V, Mohanty AK et al (2014) Analysis of Porous Electrospun Fibers from Poly(l-lactic acid)/Poly(3-hydroxybutyrate-co-3-hydroxyvalerate) Blends. Acs Sustain Chem Eng 2(8):1976–1982
13. Fergala A, AlSayed A, Khattab S et al (2018) Development of Methane-Utilizing Mixed Cultures for the Production of Polyhydroxyalkanoates (PHAs) from Anaerobic Digester Sludge. Environ Sci Technol 52(21):12376–12387
14. Zhao X, Ji K, Kurt K et al (2019) Optimal mechanical properties of biodegradable natural rubber-toughened PHBV bioplastics intended for food packaging applications. Food Packaging Shelf 21:100348. DOI: https://doi.org/10.1016/j.fpsl.2019.100348
15. Castro-Mayorga JL, Fabra MJ, Pourrahimi AM et al (2017) The impact of zinc oxide particle morphology as an antimicrobial and when incorporated in poly(3-hydroxybutyrate-co-3-hydroxyvalerate) films for food packaging and food contact surfaces applications. Food Bioprod Process 101:32–44
16. Berthet MA, Angellier-Coussy H, Chea V et al (2015) Sustainable food packaging: Valorising wheat straw fibres for tuning PHBV-based composites properties. Compos Part A-Appl S 72:139–147
17. Phromma W, R Magaraphan (2017) Fabrication of Admicelled Natural Rubber by Polycaprolactone for Toughening Poly(lactic acid). J Polym Environ 26(6):2268–2280
18. Yu H, Yan C,J Yao (2014) Fully biodegradable food packaging materials based on functionalized cellulose nanocrystals/poly(3-hydroxybutyrate-co-3-hydroxyvalerate) nanocomposites. RSC Adv 4(104):59792–59802
19. Xiang S, Feng L, Bian X et al (2019) Toughening modification of PLLA with PCL in the presence of PCL-b-PLLA diblock copolymers as compatibilizer. Polym Advan Technol 30(4):963–972
20. Zhang C, Zhang N, Wen X (2007) Synthesis and characterization of biocompatible, degradable, light-curable, polyurethane-based elastic hydrogels. J Biomed Mater Res A 82(3):637–650
21. Liu Q, Wang H, Chen L et al (2019) Enzymatic degradation of fluorinated Poly(ε-caprolactone) (PCL) block copolymer films with improved hydrophobicity. Poylm Degrad Stabil 165:27–34
22. Marcos-Fernández A, Abraham GA, Valentín JL et al (2006) Synthesis and characterization of biodegradable non-toxic poly(ester-urethane-urea)s based on poly(ε-caprolactone) and amino acid derivatives. Polymer 47(3):785–798
23. Z Sun (2019) Hyperbranched Polymers in Modifying Natural Plant Fibers and Their Applications in Polymer Matrix Composites-A Review. J Agric Food Chem 67(32):8715–8724
24. Li S, Y Yao (2019) Synergistic improvement of epoxy composites with multi-walled carbon nanotubes and hyperbranched polymers. Compos Part B-Eng 165:293–300
25. Yang J-P, Chen Z-K, Yang G et al (2008) Simultaneous improvements in the cryogenic tensile strength, ductility and impact strength of epoxy resins by a hyperbranched polymer. Polymer 49(13–14):3168–3175
26. Lu Y, Nemoto T, Tosaka M et al (2017) Synthesis of structurally controlled hyperbranched polymers using a monomer having hierarchical reactivity. Nat Commun 8(1):1863
27. Blackburn C, Tai H, Salerno M et al (2019) Folic acid and rhodamine labelled pH responsive hyperbranched polymers: Synthesis, characterization and cell uptake studies. Eur Polym J 120:109259. DOI: https://doi.org/10.1016/j.eurpolymj.2019.109259
28. Chen S, Zhang D, Jiang S et al (2012) Preparation of hyperbranched epoxy resin containing nitrogen heterocycle and its toughened and reinforced composites. J Appl Polym Sci 123(6):3261–3269
29. Sun J, Jin Y, Wang B et al (2021) High-toughening modification of polylactic acid by long-chain hyperbranched polymers. J Appl Polym Sci 138(48):e51295. DOI: https://doi.org/10.1002/app.51295
30. Smet M, Gottschalk C, Skaria S et al (2005) Aliphatic Hyperbranched Copolyesters by Combination of ROP and AB2-Polycondensation. Macromol Chem Phys 206(24):2421–2428
31. Li F, Yu HY, Li YZ et al (2021) "Soft-rigid" synergistic reinforcement of PHBV composites with functionalized cellulose nanocrystals and amorphous recycled polycarbonate. Compos Part B-Engineering 206:108542. DOI: https://doi.org/10.1016/j.compositesb.2020.108542

Publisher's Note Springer Nature remains neutral with regard to jurisdictional claims in published maps and institutional affiliations.